IEEE Access
Multidisciplinary | Rapid Review | Open Access Journal

Received December 16, 2016, accepted January 2, 2017, date of publication January 10, 2017, date of current version March 28, 2017.

Digital Object Identifier 10.1109/ACCESS.2017.2651149

A Compact Quasi-Isotropic Shorted Patch Antenna

YONG MEI PAN[1], (Member, IEEE), AND SHAO YONG ZHENG[2], (Member, IEEE)
[1]School of Electronic and Information Engineering, South China University of Technology, Guangzhou 510641, China
[2]School of Electronics and Information Technology, Sun Yat-sen University, Guangzhou 510006, China

Corresponding author: Y. M. Pan (eeympan@scut.edu.cn)

This work was supported in part by the National Natural Science Foundation of China under Grant 61302001, in part by the Guangdong Natural Science Funds for Distinguished Young Scholars under Grant 2016A030306007, and in part by the Guangdong Provincial Key Laboratory of Short Range Wireless Detection and Communication.

ABSTRACT A compact shorted patch antenna with quasi-isotropic radiation pattern is proposed in this paper. The antenna consists of a radiating patch, a small ground plane that has the same dimensions with the top patch, and a metallic sidewall which connects the former two. A coaxial probe is used to feed the antenna and excite its fundamental TEM mode, whose magnetic field generates surface electric current on the shorted sidewall and electric field generates surface magnetic current on the open-ended aperture. Due to the inherent properties of the electric and magnetic fields, the corresponding currents are found not only perpendicular but also quadrature with each other, and, therefore, the patch antenna can provide a quasi-isotropic radiation pattern without involving complex feeding circuit. To verify the theory, a prototype operating at 2.4-GHz WLAN band was designed, fabricated, and measured. Reasonable agreement between the calculated, simulated, and measured results is obtained. It has been shown that the difference between the maximum and minimum radiation power densities is ∼2 dB over the entire spherical radiating surface, and the difference can be further reduced to ∼0.9 dB by using a lower profile.

INDEX TERMS Patch antenna, isotropic antenna, complementary antenna, electric-magnetic dipoles.

I. INTRODUCTION

Due to the uniform and full coverage of signal, isotropic antennas are desirable in wireless access points (APs) and radio frequency identification (RFID) systems [1]–[8]. However, it has been indicated in [9] that an ideal isotropic antenna with absolutely uniform radiation and consistent polarization in every direction is impossible. As a result, quasi-isotropic antenna is considered in reality [1]–[8]. Generally, Quasi-isotropic radiation can be achieved by arraying a circle of unidirectional antenna elements [1], but this method involves bulky antenna configurations and complex feeding networks. Quasi-isotropic radiation can also be obtained by properly combining an electric dipole and an orthogonal magnetic dipole [2]–[5]. The former and latter provide omnidirectional radiation patterns in the H- and E- planes respectively, a three dimensional (3-D) quasi-isotropic pattern can therefore be realized when the two dipoles are fed by signals with quadrature phases and appropriate amplitudes ($\eta I_e = \pm jI_m$) [2]. The complementary concept was first used by Long to design a quasi-isotropic antenna by combining a monopole and two slots [3]. However, since a large ground plane was used in the structure, quasi-isotropic coverage was obtained only in upper half-space. Later, a printed dipole and a pair of 1.4-turn printed loops (magnetic dipole) were combined to provide a full spatial coverage, with gain difference over the entire spherical radiating surface given by 3.8 dB [4]. Its radiation efficiency, however, is only 30.4% due to severe ohmic loss. Four sequential rotated L-shaped monopoles can also provide a gain difference less than 6 dB within full space [5], but four way signals with equal amplitudes and quadrature phases of 0°, 90°, 180° and 270° are needed for exciting the monopoles and therefore a sequential-phase feeding network has to be included in the design. Recently, a quasi-isotropic dielectric resonate antenna (DRA) with small ground plane was proposed by the author and Leung [2]. The small ground plane functions simultaneously as an electric dipole, and it is combined with a magnetic dipole mode of the DRA to generate quasi-isotropic fields. The difference between the maximum and minimum radiation power densities is ∼5.6 dB.

Compared to the traditional patch antennas, quarter-wave shorted patch antenna that has a vertical shorting sidewall between the patch and ground plane shows advantages of

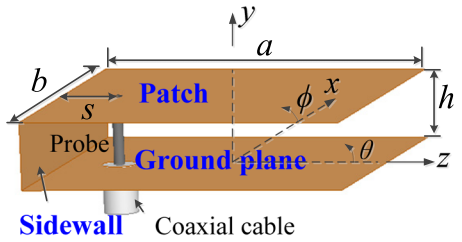

FIGURE 1. Configuration of the proposed quasi-isotropic shorted patch antenna.

smaller size [10] and wider bandwidth [11]. It has been used as an individual magnetic dipole and combined with an extra planar electric dipole to realize broadband [12]–[14] and circularly polarized (CP) antennas [15], [16]. However, thus far, almost all shorted patch antennas were developed with unidirectional [12]–[15] or omnidirectional [16] patterns. In this paper, a shorted patch antenna with quasi-isotropic radiation patterns is designed based on the complementary concept. The required equivalent magnetic and electric dipoles for obtaining the uniform pattern are provided by the transverse electric and magnetic fields of its fundamental TEM mode. Due to the inherent 90° phase difference between the electric and magnetic fields, the complementary patch antenna provides perfect isotropic coverage with gain deviation less than 2 dB over the entire spherical radiating surface. To the best of our knowledge, it is the most uniform pattern that can be obtained thus far from a singly fed antenna. For demonstration, a prototype operating at 2.4GHz has been fabricated and measured, with reasonable agreement between calculated, simulated and measured results obtained. To facilitate the design of the quasi-isotropic patch antenna, general design guidelines are summarized after a parametric study.

II. ANTENNA DESIGN

A. ANTENNA CONFIGURATION

Fig. 1 shows configuration of the proposed quasi-isotropic patch antenna, which consists of a quarter-wave rectangular radiating patch, a small ground plane, and a metallic sidewall that connects the former two. It is important to note that the top patch and ground plane have same dimensions, with their length and width given by a and b, respectively. An air substrate with thickness of h is used between them to enhance the impedance bandwidth. For exciting the antenna, the inner conductor of a coaxial cable is soldered to the patch at a displacement of s from the sidewall, whereas the outer conductor is connected to the ground plane.

B. ANTENNA MECHANISM

To explain the operating principle of the proposed antenna, the resonant E and H-fields inside the patch cavity are investigated and shown in Fig. 2. It can be seen that the E-field is mainly along the y axis, while the H-field is mainly along the x axis, indicating that it is the quasi-TEM mode. Therefore,

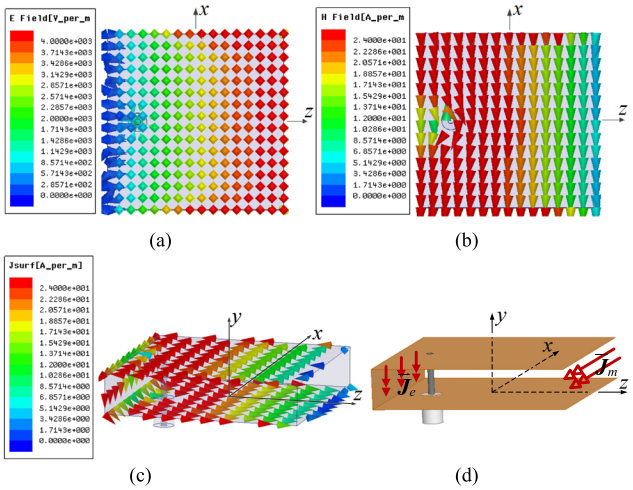

FIGURE 2. Resonant E and H-fields inside the patch cavity, and the surface current distributions on the shorted patch antenna. (a) E-field. (b) H-field. (c) Surface E-current. (d) Surface E- and M-currents.

the E-field can be expressed as [10]:

$$\vec{E} = \vec{y} E_o \sin\left(\frac{\pi z}{2a} + \frac{\pi}{4}\right) \tag{1}$$

Then, by using the Maxwell equation of $\nabla \times \vec{E} = -j\omega\mu\vec{H}$ [17], the H-fields can be obtained as:

$$\vec{H} = -\vec{x} j \frac{E_o}{\eta} \cos\left(\frac{\pi z}{2a} + \frac{\pi}{4}\right) \tag{2}$$

where η is the wave impedance of free space. The resonant frequency of the TEM mode is approximately given by [10]:

$$f = \frac{c}{2\,(2a + h)} \tag{3}$$

Assuming that the fields vanish outside the cavity, the surface electric currents on the metallic walls can be obtained by applying the boundary condition of $\vec{n} \times \vec{H} = \vec{J}_e$ [17]:

$$\vec{J}_e = \begin{cases} -\vec{z}\dfrac{jE_0}{\eta} \cos\left(\dfrac{\pi z}{2a} + \dfrac{\pi}{4}\right), & y = h \\ \vec{z}\dfrac{jE_0}{\eta} \cos\left(\dfrac{\pi z}{2a} + \dfrac{\pi}{4}\right), & y = 0 \\ -\vec{y}\dfrac{jE_0}{\eta} \cos\left(\dfrac{\pi z}{2a} + \dfrac{\pi}{4}\right) = -\vec{y}\dfrac{jE_0}{\eta}, & z = -\dfrac{a}{2} \\ 0, & otherwise \end{cases} \tag{4}$$

Similarly, the surface magnetic currents on the open-ended aperture can be obtained by using $\vec{n} \times \vec{E} = -\vec{J}_m$ [17]:

$$\vec{J}_m = \begin{cases} -\vec{z} E_0 \sin\left(\dfrac{\pi z}{2a} + \dfrac{\pi}{4}\right), & x = -\dfrac{b}{2} \\ \vec{z} E_0 \sin\left(\dfrac{\pi z}{2a} + \dfrac{\pi}{4}\right), & x = \dfrac{b}{2} \\ -\vec{x} E_0 \sin\left(\dfrac{\pi z}{2a} + \dfrac{\pi}{4}\right) = -\vec{x} E_0, & z = \dfrac{a}{2} \\ 0, & otherwise \end{cases} \tag{5}$$

With reference to (4), the surface electric currents on the patch ($y = h$) and ground plane ($y = 0$) have same amplitudes

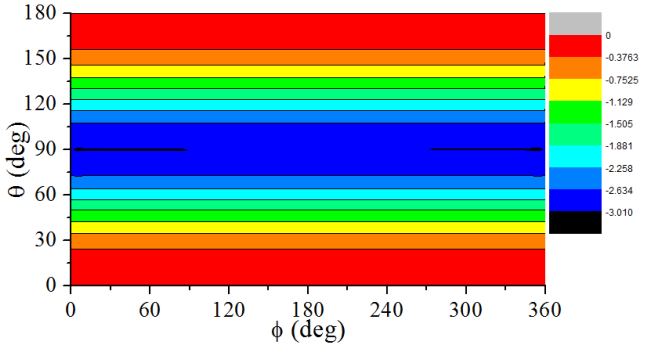

FIGURE 3. Calculated 3D radiation pattern of the shorted patch antenna.

but opposite directions. Their radiation can therefore cancel out each other when the dimensions of the ground plane and patch are comparable and the height h is much smaller than a wavelength. The same is true for the surface magnetic currents on the front ($x = -b/2$) and back ($x = b/2$) apertures. Consequently, the radiation characteristics of the shorted patch antenna can be analyzed by only considering the y-directed surface electric currents (dipole) on the shorted side-wall ($z = -a/2$) and the x-directed magnetic currents (dipole) on the open-ended aperture ($z = a/2$), as shown in Fig. 2 (d). Since the electric and magnetic currents (dipoles) are perpendicular and decoupled to each other, the far fields of the complementary dipoles can be calculated by superimposing their individual counterparts [3], [4].

$$\begin{cases} E_{T\theta} = jFbh\,(-\eta J_e \cos\theta \sin\phi + J_m \sin\phi) \\ E_{T\phi} = jFbh\,(-\eta J_e \cos\phi + J_m \cos\theta \cos\phi) \end{cases} \tag{6}$$

where $F = ke^{j\omega[t-(r/c)]}/(4\pi r)$. It can be deduced from (4) and (5) that the currents inherently satisfy the relation of $\eta J_e = -jJ_m = J$, and therefore the fields can be simplified to:

$$\begin{cases} E_{T\theta} = -FJbh \sin\phi\,(1 + j\cos\theta) \\ E_{T\phi} = -FJbh \cos\phi\,(j + \cos\theta) \end{cases} \tag{7}$$

Accordingly, the total far field is given by

$$E_T = \sqrt{|E_{T\theta}|^2 + |E_{T\phi}|^2} = FJbh\sqrt{1 + \cos^2\theta} \tag{8}$$

Fig. 3 shows theoretical normalized 3D (E_T) pattern of the shorted patch antenna. With reference to Fig. 3 and formula (8), E_T is independent of ϕ and it is only a function of θ. The difference between the maximum ($\theta = 0, \pi$) and minimum ($\theta = \pi/2$) radiation power densities is given by 3 dB, indicating that the radiation is quasi-isotropic within full space.

III. EXPERIMENT VERIFICATION

For validating the design, an isotropic shorted patch antenna covering the 2.4 GHz-WLAN band was designed, fabricated and measured. Fig. 4 shows a photograph of the prototype, which is fabricated from a U-shaped copper brick. The thickness of the copper plates is 1 mm, and the other parameters are

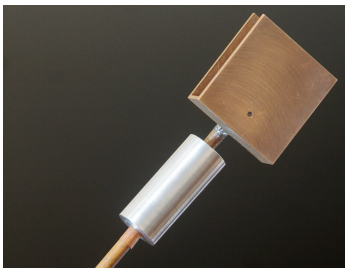

FIGURE 4. Prototype of the isotropic shorted patch antenna operating at 2.4 GHz. $a = 27$ mm, $b = 27$ mm, $h = 5.5$ mm, $s = 5$ mm.

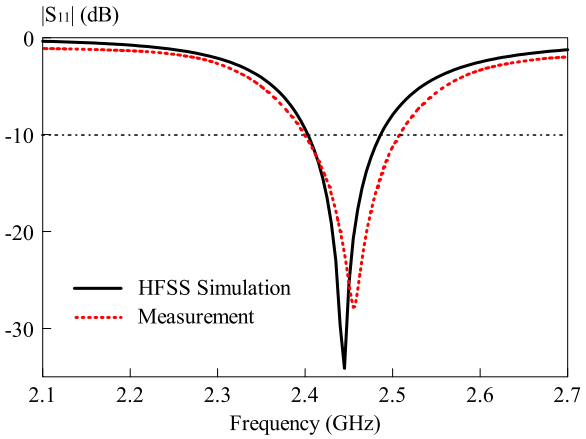

FIGURE 5. Simulated and measured reflection coefficients of the isotropic shorted patch antenna.

given by $a = 27$ mm, $b = 27$ mm, $h = 5.5$ mm, $s = 5$ mm. As shown in the figure, the feeding coaxial cable is bent to be parallel with the patch. This is because it has been found in the measurement that if the cable is located perpendicularly to the patch antenna, the current that excited outside the cable will significantly affect the antenna performance due to the small ground plane. However, the influence becomes insignificant if the cable is placed parallelly. To further suppress stay radiation from the coaxial cable, a $\lambda/4$ choke (balun) is added to the outer conductor of the cable [2]. In this paper, the reflection coefficient and radiation performance (including radiation pattern, gain and efficiency) of the antenna are measured using an HP8510C network analyzer and a Satimo StarLab System, respectively.

Fig. 5 shows simulated and measured reflection coefficients of the prototype, and good agreement between them is obtained. The simulated and measured resonant frequencies (min.$|S_{11}|$) are given by 2.44 GHz and 2.45 GHz respectively, both are a bit lower than that (2.52 GHz) of the theoretical result. This discrepancy is partially caused by the loading effect of the feeding probe, and partially due to the fringe field effect which has not been taken into account in (3). The measured 10-dB impedance bandwidth ($|S_{11}| < -10$dB) is 4.48% (2.40−2.51 GHz), comparable to that (∼5%) of a traditional patch antenna [18].

Fig. 6 shows calculated, simulated, and measured field patterns of the quasi-isotropic patch antenna in x-z and x-y planes. In each plane, the agreement between simulated

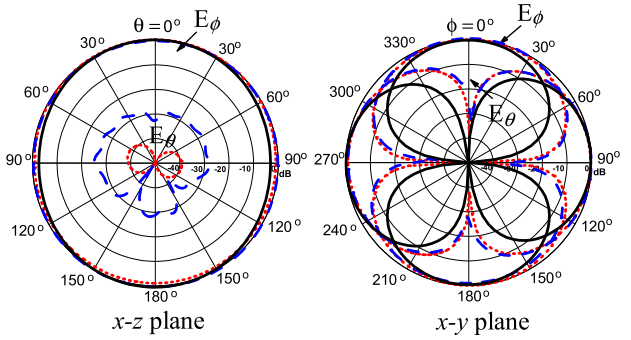

FIGURE 6. Calculated (——), simulated (.....) and measured (– – –) radiation patterns of the isotropic shorted patch antenna at 2.44 GHz.

and measured results is satisfactory, but there is a small discrepancy in the calculated pattern. This is reasonable since the above analysis is based on the assumption that the current distribution on side-walls is ideally uniform. It can be seen that the x-z plane pattern is near omnidirectional, whereas the x-y plane pattern contains two figure-8 patterns. The E_θ and E_ϕ figure-8 patterns are generated by the y-directed electric currents (dipole) and the x-directed magnetic currents (dipole), respectively. Like the quasi-isotropic DRA [2], the polarization of the fields also changes with φ, being linearly polarized when $\varphi = 0°, 90°, 180°$ and $270°$, circularly polarized when $\varphi = 45°, 135°, 225°$ and $315°$, and elliptically polarized for intermediate angles. The field patterns in the y-z plane are similar with that in the x-z plane, consistent with (7). To show more detail, Fig. 7 gives 3D pattern of the total field. Quite an isotropic pattern is observed both in the simulation and measurement, as expected. The differences between the maximum and minimum radiation power densities are given by 1.88 dB (simulation) and 1.95 dB (measurement), respectively. Compared with the theoretical pattern shown in Fig. 3, the simulated and measured patterns become more uniform due to the real current distribution. Radiation patterns are found to be very stable across the entire operating band.

Fig. 8 shows realized gains of the quasi-isotropic patch antenna at $\theta = 0°$, along with the efficiency. As can be observed from the figure, the gain and efficiency have similar trends, as expected. The measured gain varies between

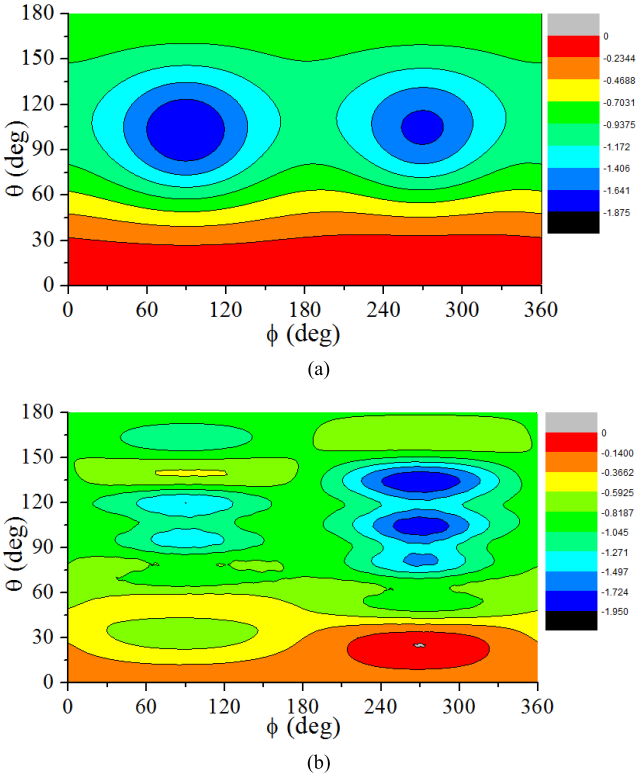

FIGURE 7. Simulated and measured 3D radiation patterns of the shorted patch antenna at 2.44 GHz. (a) Simulated. (b) Measured.

∼0.64 dBi and ∼0.93 dBi within the WLAN-band, and the average efficiency is about 90%.

A comparison between the present design and other reported isotropic antennas is summarized in Table I. From the table, it can be concluded that the proposed isotropic patch antenna outperforms most existing counterparts in the aspect of size, isotropy and efficiency.

IV. PARAMETRIC STUDY AND DESIGN GUIDELINE

A. PARAMETRIC STUDY

In this section, a parametric study of the proposed isotropic patch antenna is carried out to further characterize the design. Only one parameter is varied each time, with all the rests

TABLE 1. Comparison between the present design and other reported isotropic antennas.

Antennas	Antenna Dimensions (in terms of λ)	Impedance Bandwidth	Gain Difference	Antenna Efficiency
Present design	$0.22 \times 0.22 \times 0.06\ \lambda^3$	4.48%	1.88 dB	90%
Design in [1]	$4 \times 4 \times 8\ \lambda^3$	—	2.5 dB (over 90% of a spherical surface)	—
Design in [2]	$0.22 \times 0.22 \times 0.12\ \lambda^3$	6.9%	5.6 dB	92%
Design in [4]	$0.1 \times 0.1 \times 0.002\ \lambda^3$	0.5%	3.8 dB	30.4%
Design in [5]	$0.36 \times 0.36 \times 0.006\ \lambda^3$	20.82% (6.94% for 6dB gain deviation)	6 dB	84%
Design in [6]	$1.82 \times 1.29 \times 0.06\ \lambda^3$	15%	10.78 dB	—

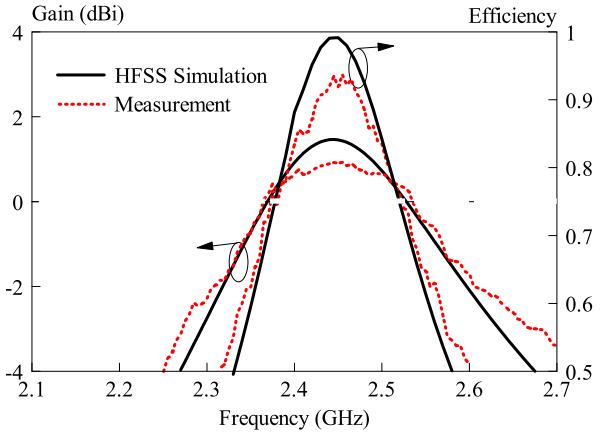

FIGURE 8. Realized gains at $\theta = 0°$ and efficiency of the shorted patch antenna.

TABLE 2. Difference between the maximum and minimum field strengths of the shorted patch antenna.

a (mm)	Difference (dB)	b (mm)	Difference (dB)	h (mm)	Difference (dB)
25	2.04	25	1.83	3.5	1.40
27	1.88	27	1.88	5.5	1.88
29	1.76	29	1.88	7.5	2.31

fixed at their optimal values as listed in Fig. 4. The effects of patch dimensions on the antenna performance are studied first. Fig. 9(a), (b) and (c) show the simulated reflection coefficients for different patch lengths, widths and heights, respectively. It can be observed that the resonant frequency shifts downward quickly from 2.56 GHz to 2.34 GHz as a increases from 25 mm to 29 mm, however it is insensitive to the variation of width b. This is because b corresponds to the dimension of non-radiating edge of the patch. The trend of reflection coefficient versus height h is similar to that of a, verifying again that the resonant frequency approximately satisfies the relation of $f = c/(4a+2h)$. It was found in HFSS study that the patch dimension also affects the distribution of radiation power density. For reference, Table II lists the difference between maximum and minimum field strengths over the entire spherical radiation surface. Again, the effect of b is much smaller than that of a and h, as expected. The field strength difference at resonant frequency changes from $\sim$ 2.3 dB to $\sim$ 1.4 dB when h decreases from 7.5 mm to 3.5 mm, indicating that a lower profile provides a more uniform radiation. This is due to the fact that the radiation caused by the patch and ground tends to be zero when they are close to each other, minimizing its effect on the isotropic pattern. To further explore the limit of isotropy, three shorted patch antennas with different heights h are designed to operate at $\sim$2.4 GHz. In each design, the dimensions of patch (a, b) and the location of feeding probe (s) are tuned to optimize the antenna. Fig. 10 shows the simulated reflection coefficients and 3D radiation patterns for the three cases, and Table III summarizes the antenna dimensions, bandwidths, and gain differences. Again, it can be seen that the gain difference decreases considerably from 3.13 dB to 0.91 dB when h varies from 10 mm to 1mm. However, the impedance bandwidth degrades from 8.16% to 0.61% accordingly. The result is reasonable because using a thinner air substrate always gives a narrower bandwidth [18]. Therefore, there is a tradeoff between radiation isotropy and impedance bandwidth. The designer has the flexibility to select the isotropic patch antenna most suitable for the intended application.

Next, the position of feeding probe is investigated and the result is shown in Fig. 11. Similar to the traditional patch antenna, the feeding position significantly affects the impedance match due to the loading effect of probe. The influence of s on the radiation pattern is also studied. It is found that the gain difference varies slightly from 1.83 dB to 1.90 dB as s increases from 3 mm to 7 mm. The results reveal that s can be used to tune the match after the isotropic pattern is optimized by tuning the patch dimensions.

As discussed above, the small ground-plane plays an important role in obtaining the isotropic radiation pattern. Therefore, the effect of different ground plane side-lengths, e.g. $g = 27$ mm, 37 mm and 67 mm is investigated in Fig. 12. As can be seen from the figure, the resonant frequency is 2.44 GHz for the antenna with $g = 27$ mm, and it moves downwards to 2.23 GHz when $g = 67$ mm. This frequency shift is caused by the fact that a good image of the patch is obtained when using a sufficiently large ground plane. The height therefore increases to $2h$ according to the image theory, and the resonant frequency is given by $f = c/(4a + 4h)$. The matching level at resonant frequency also changes with

TABLE 3. Dimensions, bandwidths and gain differences of the three different antennas operating at 2.4-GHz.

Antenna	Patch dimensions $a \times b \times h$ (mm)	Feeding position s (mm)	Impedance bandwidth	Gain difference (dB)
I	29.4 × 29.4 × 1	3.4	0.61 %	0.91
II	27 × 27 × 5.5	5.0	3.48 %	1.88
III	29.4 × 29.4 × 10	14.4	8.16 %	3.13

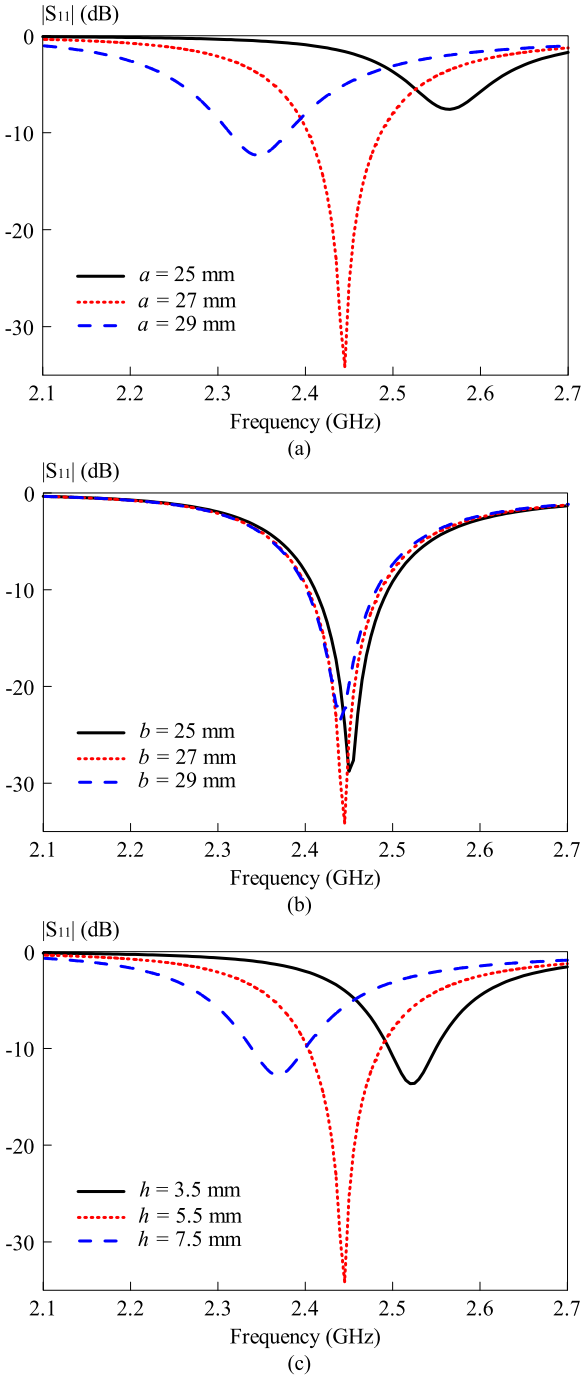

FIGURE 9. Simulated reflection coefficient of the isotropic patch antenna for different patch (a) lengths, (b) widths, and (c) heights.

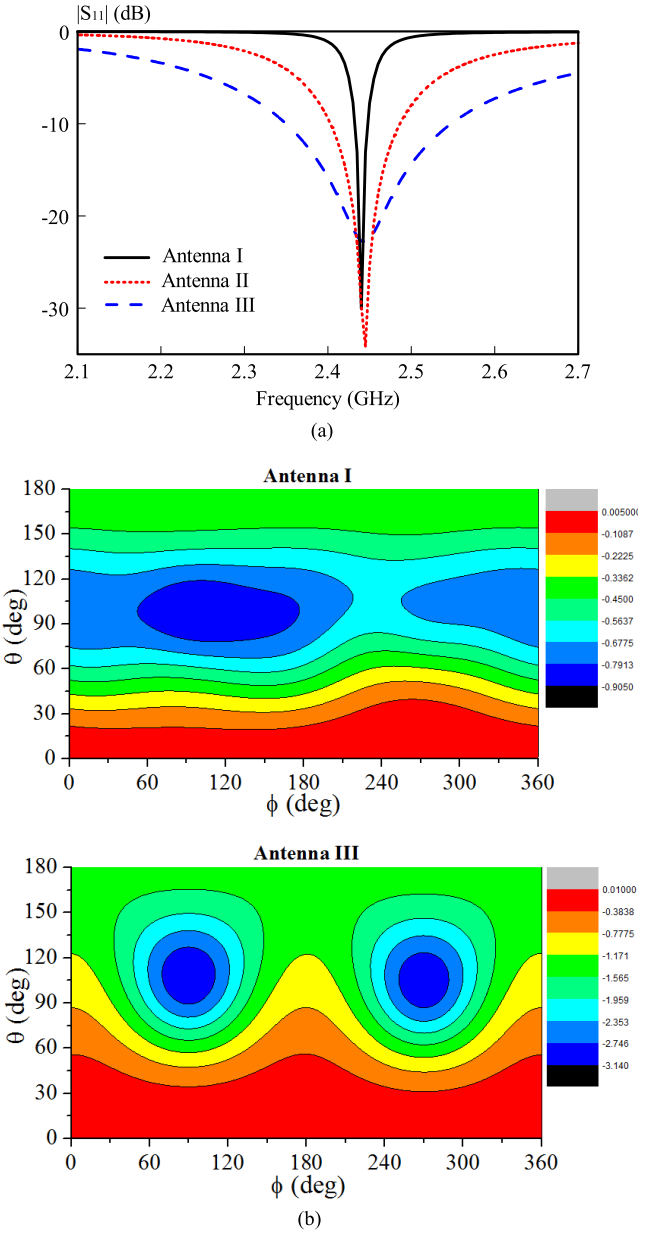

FIGURE 10. Simulated reflection coefficients and 3D radiation patterns of different isotropic patch antennas operating at 2.4-GHz. The antenna dimensions are given in Table III. (a) Reflection coefficients. (b) 3D radiation patterns of Antennas I and III (The pattern of Antenna II is shown in Fig. 7a).

the variation of g, and more importantly, significant changes have taken place in the far filed radiation patterns. Table IV compares the maximum gain, minimum gain, and the difference between them for the three antennas. An isotropic pattern is obtained when using a small ground plane (27mm), with the gain difference given by 1.88 dB. The difference increases significantly as g increasing, and even reaches 24.5 dB when $g = 67$ mm. In this case, a unidirectional pattern with maximum radiation found near y axis is resulted, and the antenna turns into a normal shorted patch antenna having large ground plane [10]. These results verify again the small ground plane is very essential to the isotropic radiation. It is worth mentioning that the function of the small ground plane is quite different from that in the previous DRA [2]. In the present design, the small ground plane is mainly used to cancel out the radiation of the patch. However, in the previous DRA [2], the small ground plane was used as an electric dipole and combined with the equivalent magnetic dipole of the DRA to generate quasi-isotropic fields. In brief, the radiation of ground is suppressed in the former and utilized in the latter.

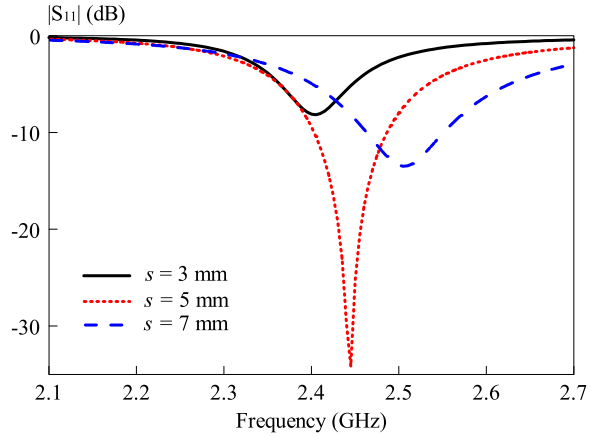

FIGURE 11. Simulated reflection coefficient of the isotropic patch antenna for different positions of the feeding probe.

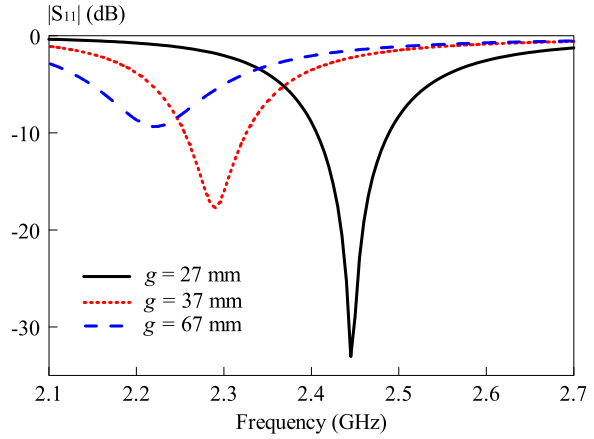

FIGURE 12. Simulated reflection coefficient of the shorted patch antenna for different side-lengths of the ground plane.

TABLE 4. Maximum and minimum field strengths of the shorted patch antenna with different ground planes

Ground size (mm^2)	Max. field strength (dB)	Min. field strength (dB)	Difference (dB)
27×27	1.47	-0.41	1.88
37×37	2.48	-2.73	5.21
67×67	4.04	-20.47	24.51

B. DESIGN GUIDELINE

Based on the parametric study, a simple guideline is given to facilitate the design of the proposed isotropic patch antenna. It is assumed that the design wavelength is λ_0.

1) Firstly, setting the initial dimensions of the patch as $a = b = 0.25\lambda_0$, and $h = 0.04\ \lambda_0$ (a larger h can be chosen if wider bandwidth is required). Using a ground plane as large as the patch ($g = 0.25\lambda_0$).
2) Then, inserting a coaxial probe near the metallic side-wall to feed the antenna.
3) Tuning dimensions of the patch to optimize the isotropic pattern, and adjusting the feeding position for good match.
4) Repeating procedure (3) until satisfying performance is achieved.

V. CONCLUSION

A probe-fed shorted patch antenna with isotropic radiation pattern is investigated in this paper. The antenna uses a small ground plane which has same dimensions with the patch, therefore the radiation caused by the currents on the patch is cancelled out by that comes from the opposite currents on the ground plane. Quasi-TEM mode is excited in the patch cavity, generating surface magnetic current on the open-ended aperture and electric current on the shorted side-wall. Taking advantage of the inherent properties of the orthogonal electric and magnetic fields (currents), the shorted patch antenna provides an isotropic radiation pattern without using complex feeding circuit. A 2.4-GHz prototype was designed and measured to verify the theory. Uniform radiation with gain difference of 1.95 dB is obtained over the entire spherical radiating surface. It has been found that there is a trade-off between radiation isotropy and impedance bandwidth. By tuning the height of the patch, an antenna with different bandwidths (from 8% to 0.6%) and gain differences (from 3.1 to 0.9 dB) can be obtained.

REFERENCES

[1] Z. Zhang, X. Gao, W. Chen, Z. Feng, and M. F. Iskander, "Study of conformal switchable antenna system on cylindrical surface for isotropic coverage," *IEEE Trans. Antennas Propag.*, vol. 59, no. 3, pp. 773–776, Mar. 2011.
[2] Y. M. Pan, K. W. Leung, and K. Lu, "Compact quasi-isotropic dielectric resonator antenna with small ground plane," *IEEE Trans. Antennas Propag.*, vol. 62, no. 2, pp. 577–585, Feb. 2014.
[3] S. Long, "A combination of linear and slot antennas for quasi-isotropic coverage," *IEEE Trans. Antennas Propag.*, vol. 23, no. 4, pp. 572–576, Jul. 1975.
[4] X. J. Xu, H. C. Huang, and Y. X. E. Wang, "Isotropic radiation from an electrically small loop-loaded printed dipole," in *Proc. IEEE Int. Workshop Antenna Tech. (iWAT)*, Mar. 2009, pp. 1–4.
[5] C. J. Deng, Y. Li, Z. J. Zhang, and Z. H. Feng, "A wideband isotropic radiated planar antenna using sequential rotated L-shaped monopoles," *IEEE Trans. Antennas Propag.*, vol. 62, no. 3, pp. 1461–1464, Mar. 2014.
[6] L. Pazin, A. Dyskin, and Y. Leviatan, "Quasi-isotropic X-band inverted-F antenna for active RFID tags," *IEEE Antennas Wireless Propag. Lett.*, vol. 8, pp. 27–29, 2009.
[7] H. K. Ryu, G. Jung, D. K. Ju, S. Lim, and J. M. Woo, "An electrically small spherical UHF RFID tag antenna with quasi-isotropic patterns for wireless sensor networks," *IEEE Antennas Wireless Propag. Lett.*, vol. 9, pp. 60–62, 2010.
[8] A. Mehdipour, H. Aliakbarian, and J. Rashed-Mohassel, "A novel electrically small spherical wire antenna with almost isotropic radiation pattern," *IEEE Antennas Wireless Propag. Lett.*, vol. 7, pp. 396–399, 2008.
[9] H. F. Mathis, "A short proof that an isotropic antenna is impossible," in *Proc. IRE*, vol. 39. 1951, p. 970.
[10] S. Pinhas and S. Shtrikman, "Comparison between computed and measured bandwidth of quarter-wave microstrip radiators," *IEEE Trans. Antennas Propag.*, vol. 36, no. 11, pp. 1615–1616, Nov. 1988.
[11] J. S. Row and Y.-Y. Liou, "Broadband short-circuited triangular patch antenna," *IEEE Trans. Antennas Propag.*, vol. 54, no. 7, pp. 2137–2141, Jul. 2006.
[12] K. M. Luk and B. Q. Wu, "The magnetoelectric dipole—A wideband antenna for base stations in mobile communications," *Proc. IEEE*, vol. 100, no. 7, pp. 2297–2307, Jul. 2012.
[13] K. M. Luk and H. Wong, "A new wideband unidirectional antenna element," *Int. J. Microw. Opt. Technol.*, vol. 1, no. 1, pp. 35–44, Jun. 2006.
[14] L. Ge and K. M. Luk, "A low-profile magnetoelectric dipole antenna," *IEEE Trans. Antennas Propag.*, vol. 60, no. 4, pp. 1684–1689, Apr. 2012.

[15] W. H. Zhang, W. J. Lu, and K. W. Tam, "A planar end fire circularly polarized complementary antenna with beam in parallel with its plane," *IEEE Trans. Antennas Propag.*, vol. 64, no. 3, pp. 1146–1152, Mar. 2016.
[16] J. H. Liu, Y. X. Li, Z. X. Liang, and Y. L. Long, "A planar quasi magnetic-electric circularly polarized antenna," *IEEE Trans. Antennas Propag.*, vol. 64, no. 6, pp. 2108–2114, Jun. 2016.
[17] D. M. Pozar, *Microwave Engineering*, 3rd ed. Hoboken, NJ, USA: Wiley, 2005.
[18] K. F. Lee and K. M. Luk, *Microstrip Patch Antennas*. Singapore: World Scientific, 2011.

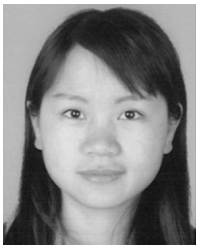

YONG MEI PAN (M'11) was born in Huangshan, China. She received the B.Sc. and Ph.D. degrees in electrical engineering from the University of Science and Technology of China, Hefei, China, in 2004 and 2009, respectively. From 2009 to 2012, she was a Research Fellow with the Department of Electronic Engineering, City University of Hong Kong, Hong Kong. In 2013, she joined the School of Electronic and Information Engineering, South China University of Technology, Guangzhou, China, as an Associate Professor, where she is currently a Professor. Her research interests include dielectric resonator antennas, leaky wave antennas, metasurface antennas, and filtering antennas.

Prof. Pan is currently an Associate Editor of the IEEE Transactions on Antennas and Propagation.

SHAO YONG ZHENG (S'07–M'11) was born in Fujian, China. He received the B.S. degree from Xiamen University, Fujian, China, in 2003, and the M.Sc., M.Phil., and Ph.D. degrees from the City University of Hong Kong, Hong Kong, in 2006, 2008, and 2011 respectively, all in electronic engineering.

From 2011 to 2012, he was a Research Fellow with the Department of Electronic Engineering, City University of Hong Kong. He is currently an Associate Professor with the Department of Electronics and Communication Engineering, Sun Yat-sen University, Guangzhou, China. His research interests include microwave/millimeter wave circuits and evolutionary algorithms.